Supporting Information

A Highly Selective Ratiometric Chemosensor for Ni^{2+} in Quinoxaline Matrix

Shyamaprosad Goswami*[a], Shampa Chakraborty[a], Monoj Kumar Adak[a], Sandipan Halder[b] , Ching Kheng Quah[c] , Hoong-Kun Fun[c,d], Bholanath Pakhira[a], Sabyasachi Sarkar[a]

TABLE OF CONTENTS

1. Experimental Section :

A single crystal of **HOQA** suitable for X-ray crystallography was obtained by solvent diffusion method using methanol and chloroform (Fig. 7).

2. General procedure for drawing Job plot by UV–vis method:

Stock solution of same concentration of sensor and Ni were prepared in the order of ≈ 1.0 x 10^{-5} ML^{-1} CH_3CN . The absorbance in each case with different *host–guest* ratio but equal in volume was recorded. Job plots were drawn by plotting $\Delta I.X_{host}$ *vs* X_{host} (ΔI = change of intensity of the absorbance spectrum during titration and X_{host} is the mole fraction of the host in each case, respectively).

3. Determination of Detection Limit:

The detection limit DL of **HOQA** for Ni^{+2} was determined from the following equation[1]:

DL = K* Sb1/S

Where K = 2 or 3 (we take 3 in this case); Sb1 is the standard deviation of the blank solution; S is the slope of the calibration curve.

From the graph we get slope = 8994 , and Sb1 value is. 0.015254564, Thus using the formula we get the Detection Limit = 5.59 µM i.e. **HOQA** can detect Ni^{2+} in this minimum concentration.

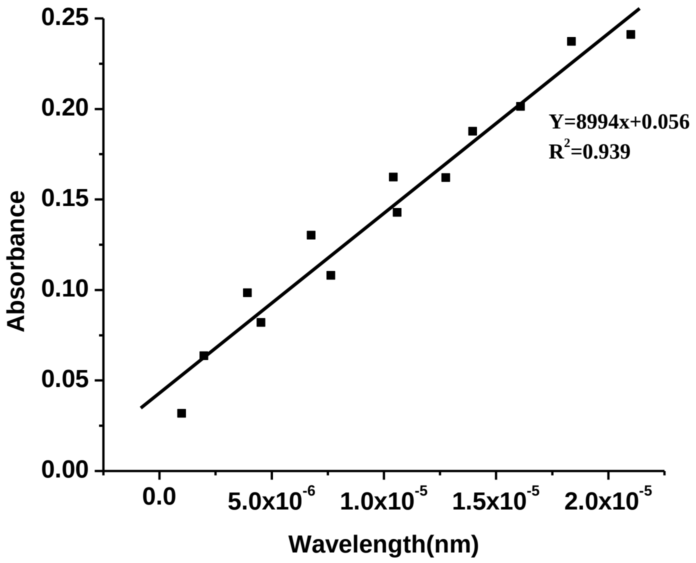

Figure S1: Absorbance vs Conentration plot of receptor **HOQA** ($1x10^{-5}$M) with Ni^{2+}.

4. Determination of Association constant:

The association constants were calculated based on the titration curve of the probes with metal ions. Association constants were determined by a nonlinear least squares fit of the data with the following equation. [2]

$$I = (I_0 + K_1 \cdot C_G \cdot I\,[1{:}1] + K_1 \cdot K_2 \cdot I_{\text{lim}} \cdot C_{G2}) / (1 + K_1 \cdot C_G + K_1 \cdot K_2 \cdot C_{G2}) \qquad (1)$$

I represents the absorbance intensity, I_0 represents the intensity of pure host, and $I_{[1:1]}$ represents intensity at [G]/[H] = 1:1. C_G is the corresponding concentration of the guest and K is the association constant. The association constant and correlation coefficients (R) were obtained by a nonlinear least-square analysis of I vs. C_G.

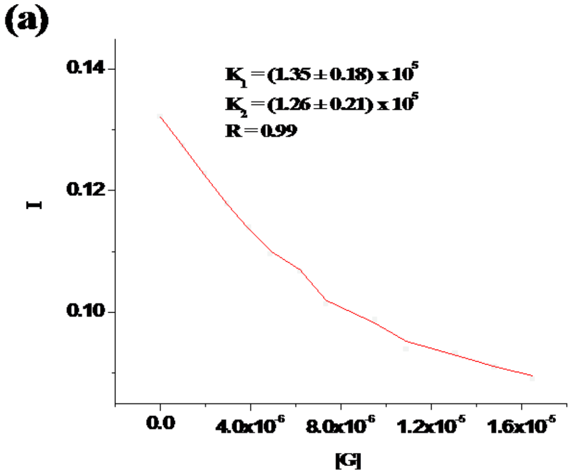

Figure S2: Plots of absorbance at 385 nm of **HOQA** as a function of [G].

5. Absorbance vs. pH plot :

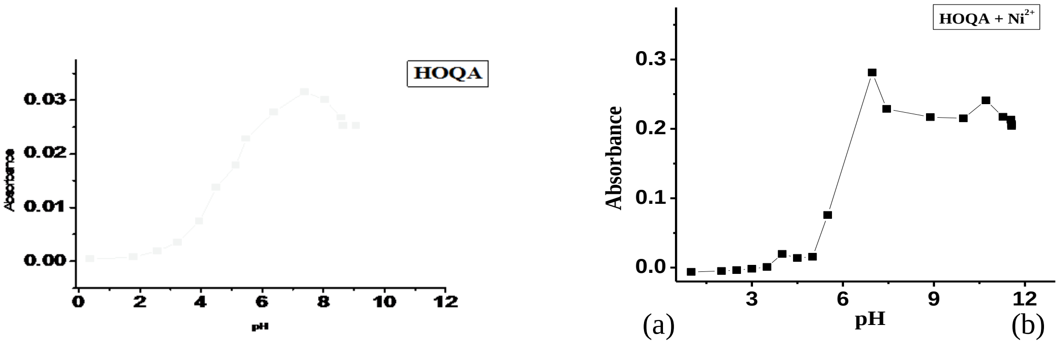

Figure S3: (a) Plots of absorbance at 385 nm of **HOQA** as a function of pH. The solid line is the best fit pH titration curve with **p*Ka*** 5.26. (b)Absobance intensity of **HOQA** (10 µM) at various pH values in CH_3CN-H_2O (9:1, v/v) medium in presence of Ni^{2+} (2.0 equiv., 2.0 x10^{-4} M) at 385nm.

6. Absorbance vs Concentration plot

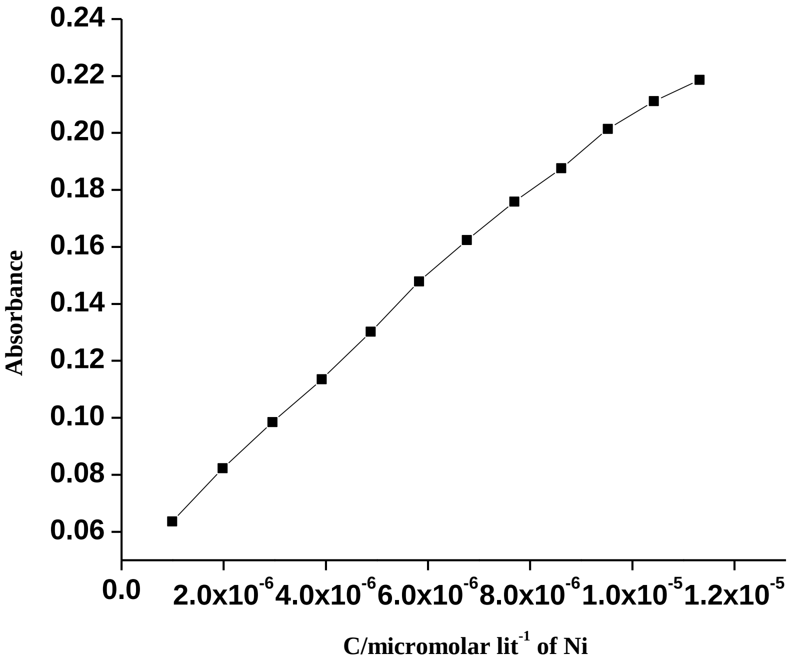

Figure S4: The change of absorbance as a function of $[Ni^{2+}]$ at 385 nm

7. Electronic spectra of free $NiCl_2$ and adding the ligand (HOQA) into it in acetonitrile medium:

The d-d absorption of Ni ion in acteonitrile appears a weak broad band around 660 nm and on adding HOQA into it two new weak absorptions appeared around 580 and 680 nm . The band around 660 nm with less intensity remained (Fig S5 (A) and (B)) due to the less equivalent addition of HOQA. These new absorptions are related to weak d-d transitions from distorted tetrahedral geometry (see text).

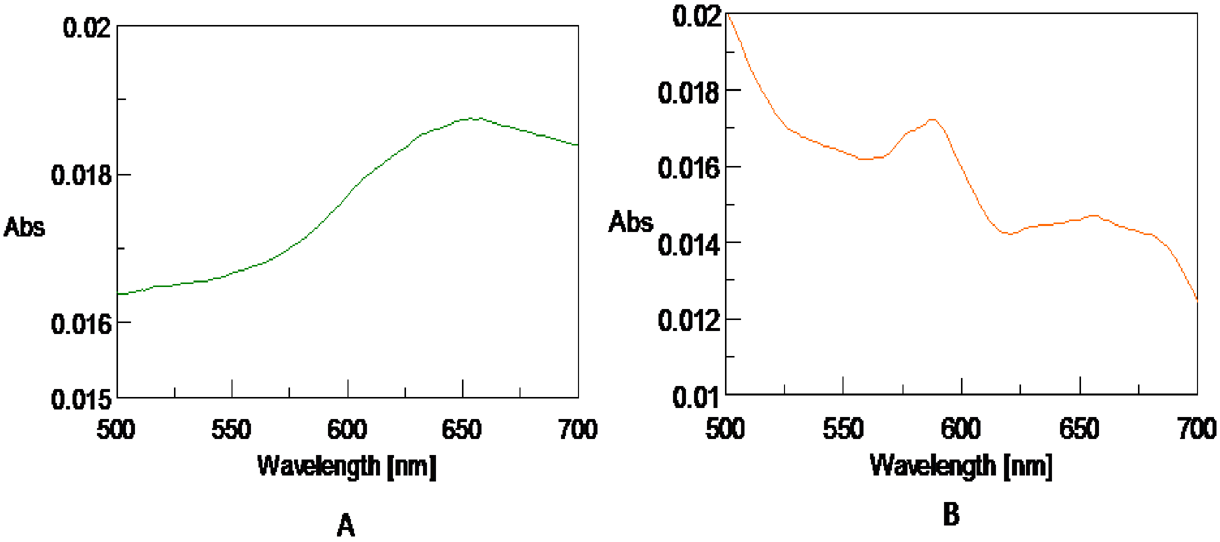

Fig: S5: Solution spectra of (A) $NiCl_2$ and (B) adding HOQA into it in acetonitrile

8. ^{1}H NMR, ESI MS and FT-IR spectra of receptor and receptor + Ni:

^{1}H NMR of Receptor:

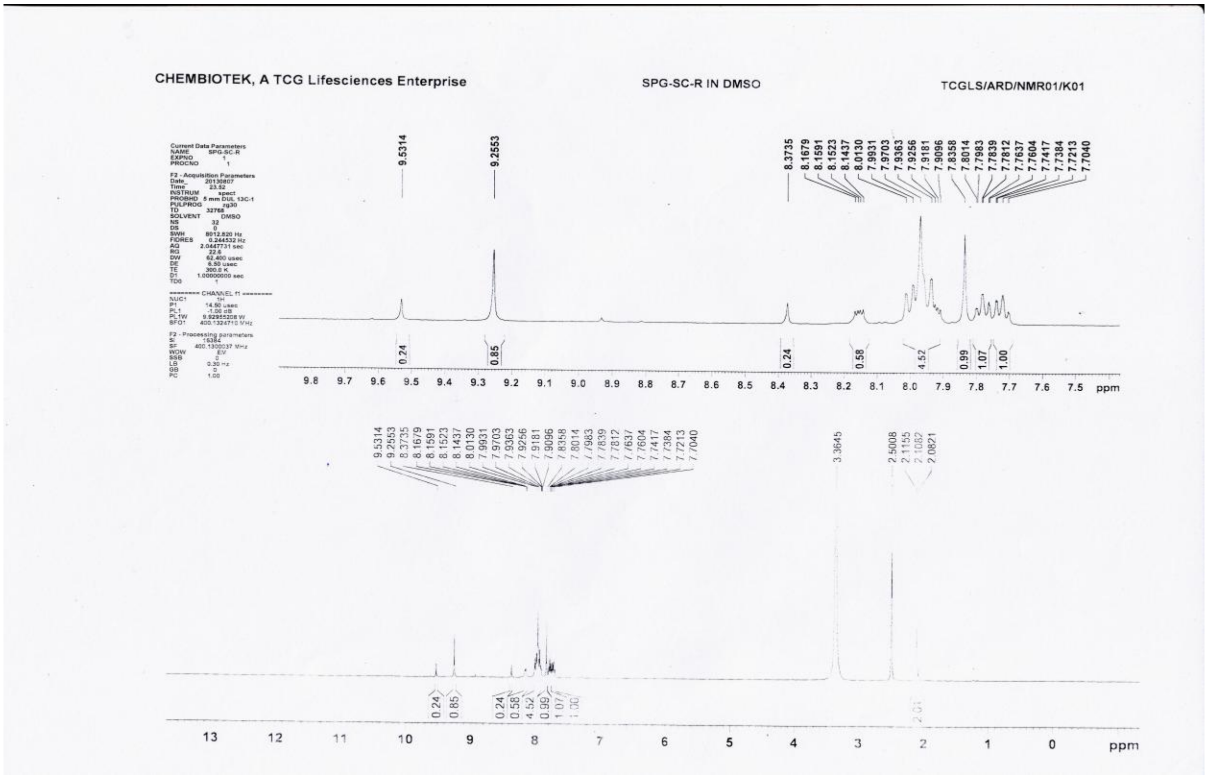

^{13}C NMR of Receptor :

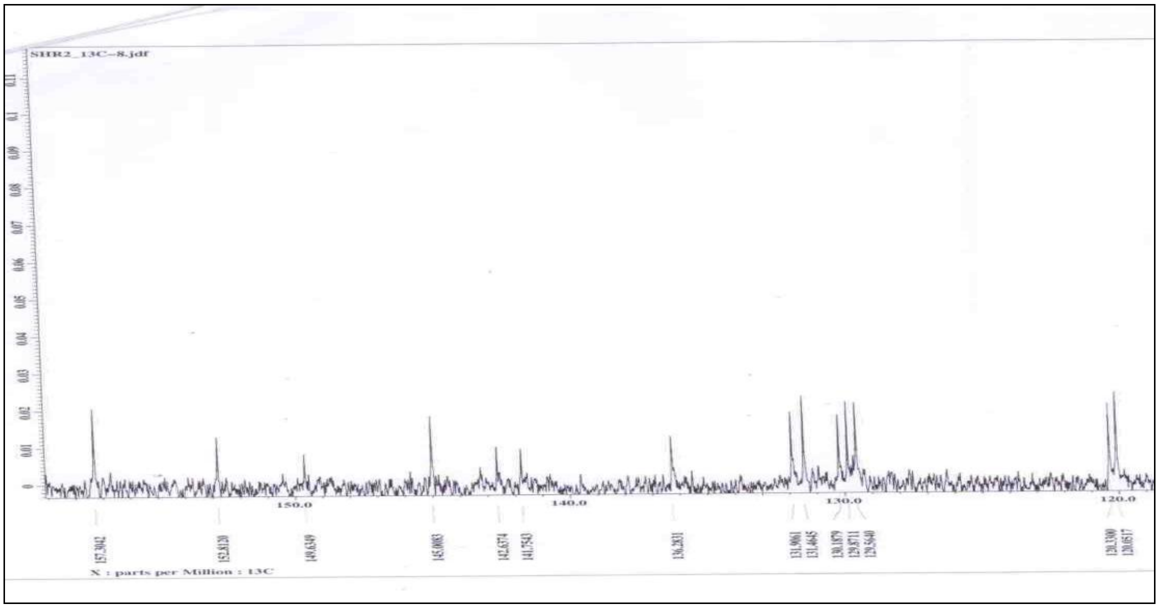

ESI LCMS spectra of Receptor:

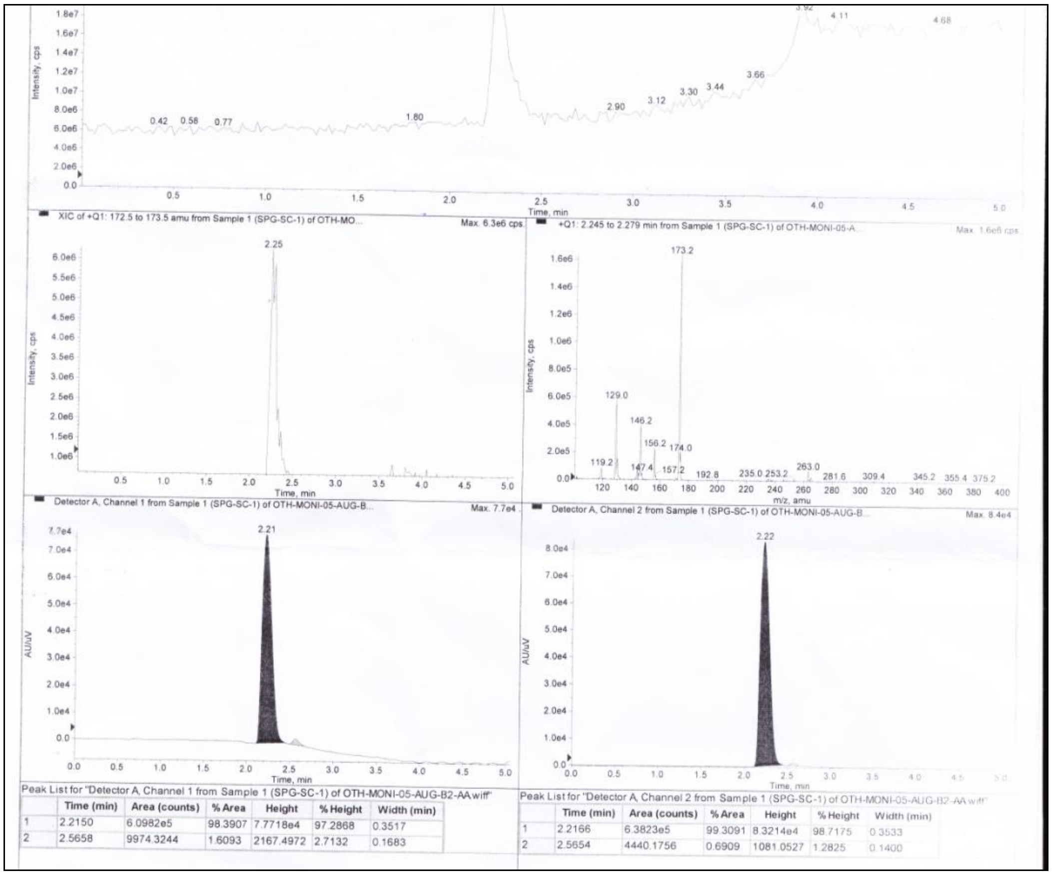

Peak List for "Detector A, Channel 1 from Sample 1 (SPG-SC-1) of OTH-MONI-05-AUG-B2-AA.wiff"

	Time (min)	Area (counts)	% Area	Height	% Height	Width (min)
1	2.2150	6.0982e5	98.3907	7.7718e4	97.2868	0.3517
2	2.5658	9974.3244	1.6093	2167.4972	2.7132	0.1683

Peak List for "Detector A, Channel 2 from Sample 1 (SPG-SC-1) of OTH-MONI-05-AUG-B2-AA.wiff"

	Time (min)	Area (counts)	% Area	Height	% Height	Width (min)
1	2.2166	6.3823e5	99.3091	8.3214e4	98.7175	0.3533
2	2.5654	4440.1756	0.6909	1081.0527	1.2825	0.1400

ESI HRMS spectra of Receptor:

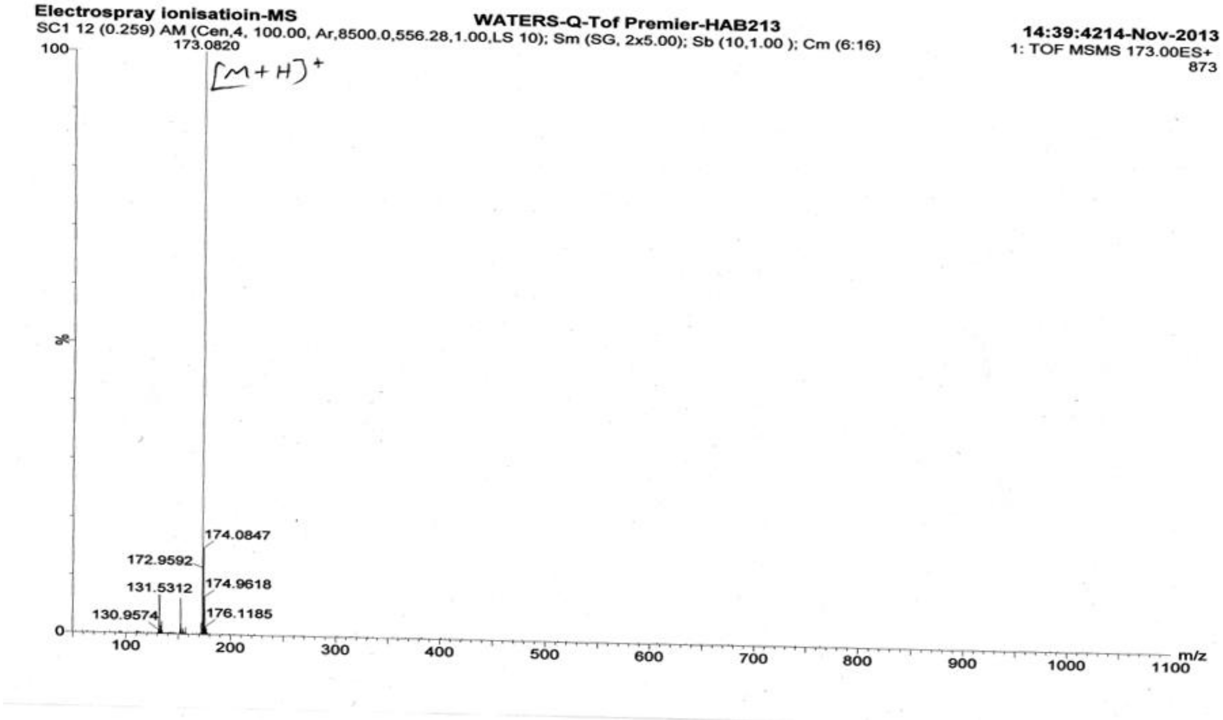

ESI LCMS spectra of receptor +Ni:

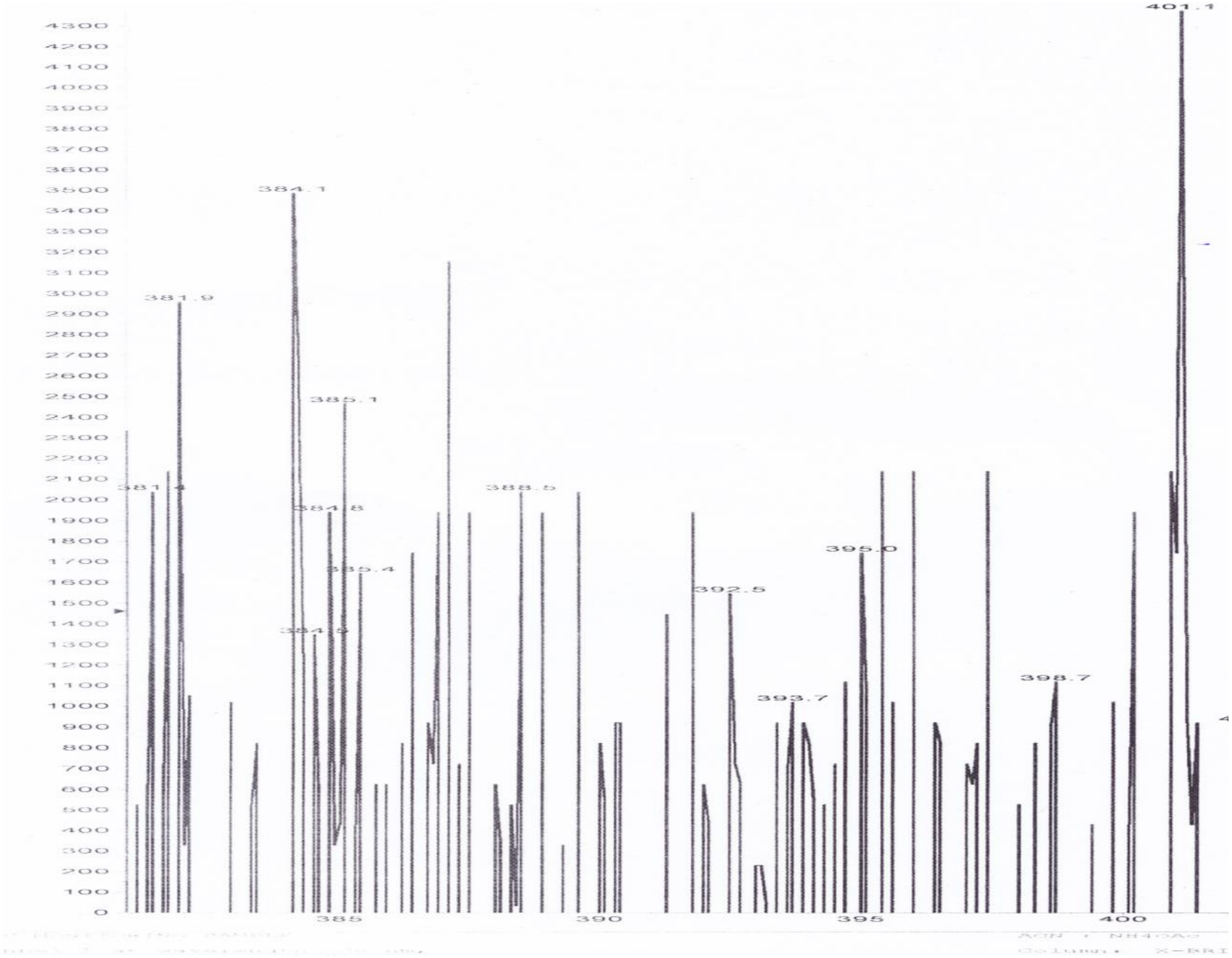

ESI HRMS spectra of receptor +Ni:

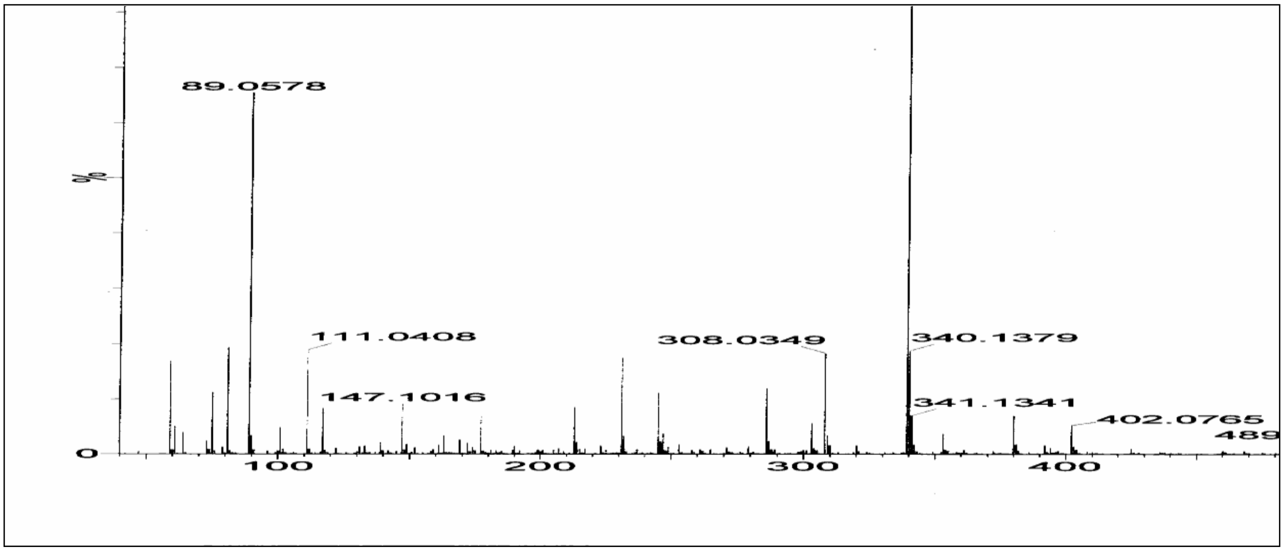

FT-IR data of (a) Receptor and its (b) Receptor +Ni

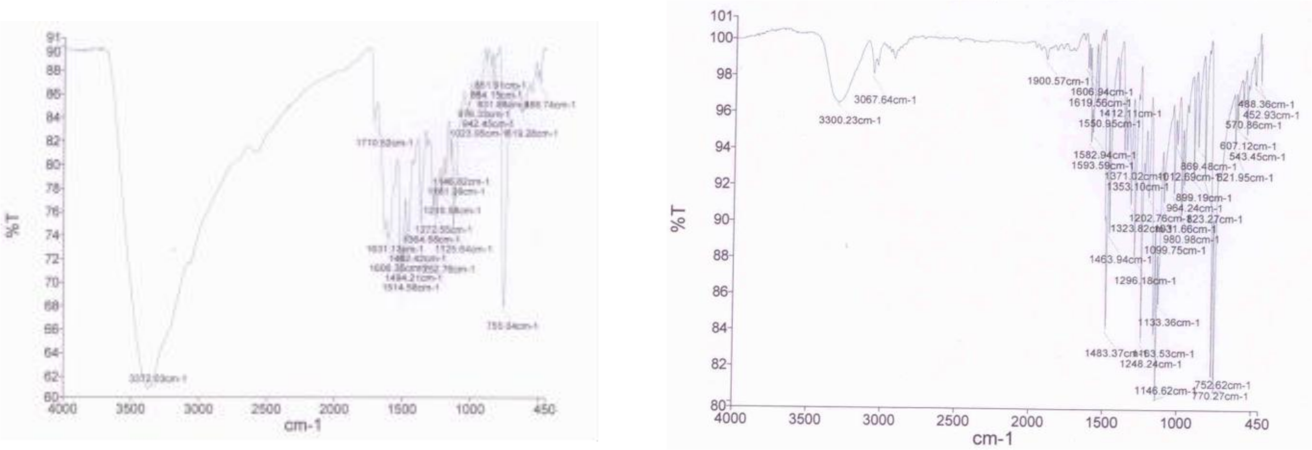

(a) (b)

9. NMR Titration spectra of receptor and receptor +Ni (0.2 equivalent and 0.5 equivalent) respectively:

a. NMR spectra of receptor (HOQA) in DMSO-d^6

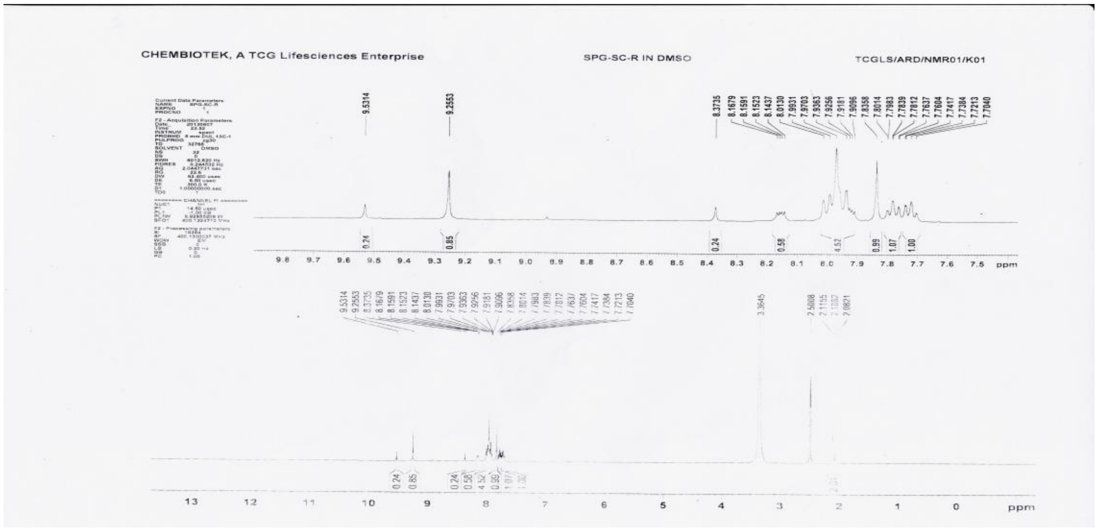

b. NMR spectra of receptor (HOQA)+Ni^{2+} (0.2 equiv) in DMSO-d^6

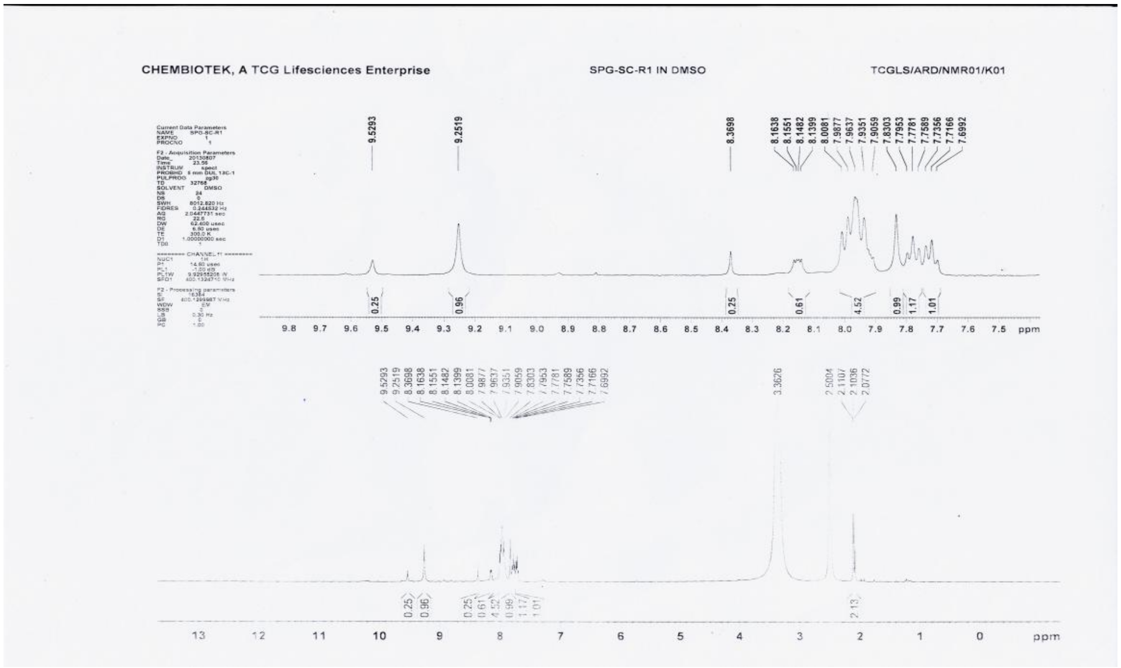

c. NMR spectra of receptor (HOQA)+Ni^{2+} (0.5 equiv) in DMSO-d^6

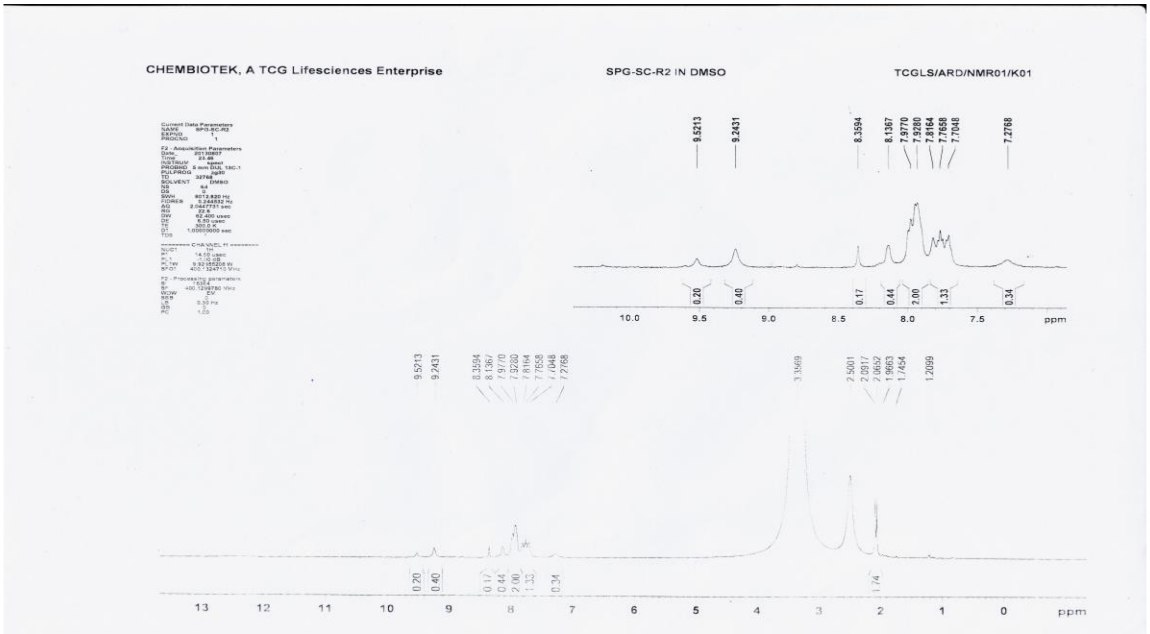

10. UV-vis spectra of receptor (HOQA) in CH_3CN-HEPES buffer (9:1, v/v, pH=7.4) .

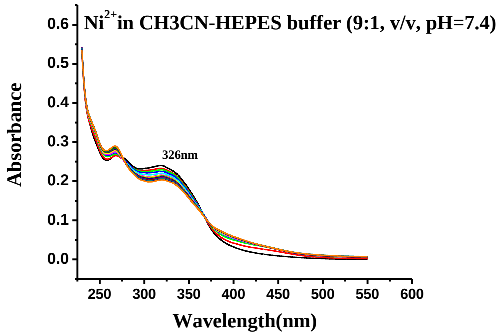

Fig: S6: spectra of HOQA in acetonitrile-HEPES buffer(9:1, v/v, pH=7.4)

11.Fluorescence titration curve of receptor (HOQA) with Ni^{2+}:

Fluorescence titration spectra of receptor ($c = 1.0 \times 10^{-5}$ M) with Ni^{2+} i.e. ($c = 2.0 \times 10^{-4}$ M) in CH_3CN.

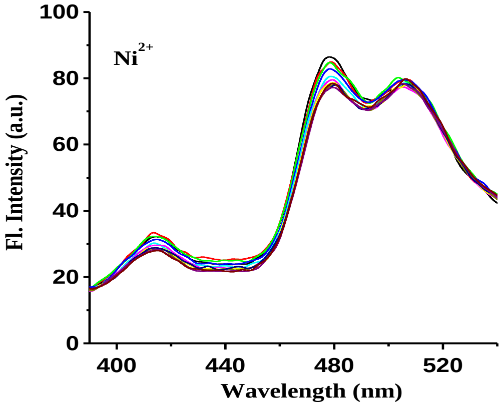

Fig: S7: spectra of HOQA in acetonitrile-HEPES buffer(9:1, v/v, pH=7.4)

12. Crystal Data

Experimental details

Crystal data	
Chemical formula	$C_9H_8N_4$
M_r	172.19
Crystal system, space group	Monoclinic, $P2_1$
Temperature (K)	100
a, b, c (Å)	7.3136 (13), 4.5404 (8), 12.823 (2)
β (°)	103.900 (4)
V (Å^3)	413.35 (13)
Z	2
Radiation type	Mo $K\alpha$
μ (mm^{-1})	0.09
Crystal size (mm)	0.73 × 0.10 × 0.05

Data collection	
Diffractometer	Bruker *SMART APEX* II DUO CCD area-detector diffractometer
Absorption correction	Multi-scan (*SADABS*; Bruker, 2009)
T_{min}, T_{max}	0.937, 0.996
No. of measured, independent and observed [$I > 2\sigma(I)$] reflections	6873, 1072, 978
R_{int}	0.040
$(\sin \theta/\lambda)_{max}$ (Å^{-1})	0.652
Refinement	
$R[F^2 > 2\sigma(F^2)]$, $wR(F^2)$, S	0.033, 0.085, 1.10
No. of reflections	1072
No. of parameters	126
No. of restraints	1
H-atom treatment	H atoms treated by a mixture of independent and constrained refinement
$\Delta\rho_{max}$, $\Delta\rho_{min}$ (e Å^{-3})	0.24, −0.18

X-ray structure analysis:

The data were collected using a Bruker APEX2 DUO CCD diffractometer with the graphite monochromated MoKα radiation at a detector distance of 5cm and with APEX2 software. The collected data were reduced using SAINT program and the empirical absorption corrections were performed using the SADABS program. The structure were solved by direct methods and refined by least-squares using the SHELXTL software package. N-bound H atoms were located in the difference Fourier map and refined freely [N—H = 0.90(2) and 0.93(2) Å]. The remaining H atoms were placed in calculated positions with C—H = 0.95 Å after checking their positions in the Fourier difference map. The U_{iso} values were constrained to be 1.2 U_{eq} of the carrier atom. 746 Fridels pairs have been merged. The crystallographic data and hydrogen bonds geometry are presented in Table 1 and 2, respectively. Crystallographic data for receptor HOQA has been deposited with the Cambridge Crystallographic Data Center No. CCDC 956036.

Table 2
Hydrogen-bond geometry (Å, º)

D—H···A	D—H	H···A	D···A	D—H···A
N4—H2*N*4···N1^{i}	0.90 (2)	2.18 (2)	3.054 (2)	165 (3)
N4—H1*N*4···N3^{ii}	0.94 (2)	2.11 (2)	3.029 (2)	166 (2)

Symmetry codes: (i) $-x, y+1/2, -z$; (ii) $-x-1, y+1/2, -z$.

13. Computational details:

Gaussian 03 package were used for the Density Functional Theory (DFT) calculations and with the help of "Gauss View" the visualization of Molecular orbitals were performed. The method used was Becke's threeparameterhybrid-exchange functional, the nonlocal correlation provided by the Lee, Yang, and Parr expression, and the Vosko,Wilk, and Nuair 1980 local correlation functional (III) (B3LYP).** The 6-311+G(d,p)basis set was used for calculations. Single-point energy calculations were done in the gas phase.

The ligand geometry was taken form X-ray crystal structure and without further optimization it was used for calculations but for the complex species the structure were optimized with B3LYP functional and 6-311+G(d,p)basis with no symmetry constrain. Time-dependent DFT (TD-DFT)calculations were also carried out using the same functional in gas phase. For ligand TD-DFT calculations, singlet excited states were calculated based on the singlet ground state geometry but for complex, triplet excited states were calculated based on the triplet ground state geometry.

Form TD-DFT calculations, the electronic transition was observed from HOMO to LUMO and HOMO to LUMO +1 at 327.08 and 275.03 nm respectively with very strong oscillator strength (f)=0.2460 and 0.5341 respectively which are very close to our experimental value.

For complex, the peak at 367.04 nm has been observed due to HOMO to LUMO transition of alpha orbitals with relatively low oscillator strength (f) =0.12.

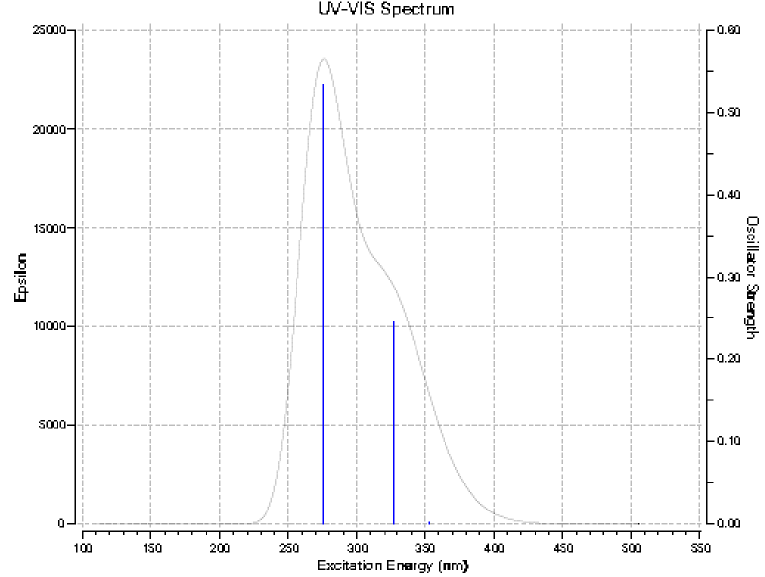

Figure S7: **Theoretically calculated electronic spectra of receptor(HOQA).**

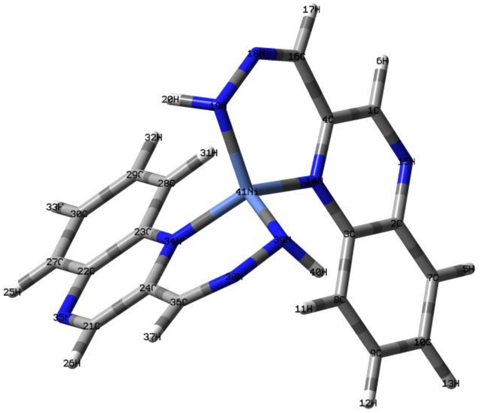

Figure S8: Optimized geometry of Ni^{2+} complex.

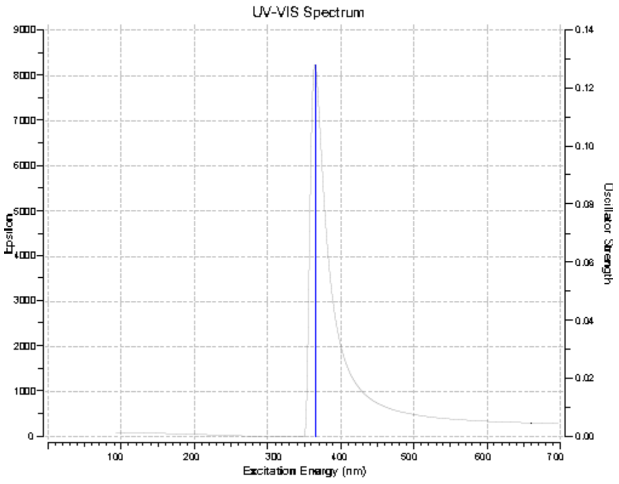

Figure S9: Electronic spectra of complex obtained form calculation.

Coordinates of optimized geometry of complex.

C	3.18697800	1.25400900	1.41317000
C	3.19631000	0.81573400	-0.84171800
C	2.05464900	-0.00823700	-0.69484200
C	2.07539400	0.40815200	1.58913400
H	4.65830200	1.60963000	-2.20407300
H	3.61997200	1.75061700	2.26320900
C	3.78999000	0.98442500	-2.10469600
C	1.52079200	-0.63878100	-1.83554500
C	2.11668400	-0.46282300	-3.08336100
C	3.25405500	0.34718100	-3.21912700
H	0.64852100	-1.25382300	-1.74870500
H	1.70034900	-0.95040200	-3.94609300
H	3.71016000	0.47852800	-4.18354900
N	1.49039900	-0.16294600	0.53163800
N	3.72385700	1.44966500	0.21696000
C	1.60119800	0.16096600	3.02211500
H	2.14484000	0.66823600	3.79880000
N	0.63078900	-0.61327200	3.40779100
N	-0.39743500	-1.13950000	2.62295000
H	-1.22493200	-0.60410500	2.83119700
C	-3.55268700	-0.76074200	-1.35084000
C	-3.04981000	1.37711100	-0.68003200
C	-1.88761400	0.90739900	-0.02105100
C	-2.39997000	-1.25115200	-0.71051800
H	-4.25588400	3.09076800	-1.16137800
H	-4.20353500	-1.44031800	-1.87153000
C	-3.37234000	2.74507600	-0.65690200
C	-1.07354500	1.83121900	0.65996900
C	-1.40335800	3.18504900	0.67706400

C	-2.55278300	3.64449700	0.01682200
H	-0.19697400	1.49643200	1.17099400
H	-0.77260200	3.88032900	1.20062200
H	-2.80247100	4.68987400	0.03319900
N	-1.58661800	-0.41724600	-0.05131400
N	-3.86067800	0.52902400	-1.33005300
C	-2.13250300	-2.75714300	-0.80275600
H	-2.90002900	-3.35198700	-1.26430400
N	-1.08081300	-3.39606400	-0.38146000
N	0.12155800	-2.82982500	0.04792700
H	0.74313300	-2.81418000	-0.74385300
Ni	-0.08517500	-1.13857500	0.78975300

14.References:

1. M. Zhu, M. Yuan, X. Liu, J. Xu, J. Lv, C. Huang, H. Liu, Y. Li, S. Wang, D. Zhu, *Org. Lett*, **2008, 10**, 1481.

2. S. Fukuzumi, Y. Kondo, S. Mochizuki, T. Tanaka, *J. Chem. Soc. Perkin Trans.*, **1989, *2***, 1753.
3. J. Cosier, A. M. Glazer, *J. Appl. Cryst*.1986, **19**, 105.

4. Bruker. APEX2, SAINT and SADABS. Bruker AXS Inc.: Madison, WI, USA, 2009.4.G.M.

5. Sheldrick, *Acta Cryst*. **2008, A64**, 112.